

---

## Compact UWB filter with narrow notched band based on grounded circular patch resonator

---

Mona Yazdani Shavakand and  
Javad Ahmadi-Shokouh\*

Faculty of Engineering,  
University of Sistan and Baluchestan,  
Zahedan, Iran  
Email: mona.yazdani.sh@gmail.com  
Email: shokouh@ece.usb.ac.ir  
\*Corresponding author

**Abstract:** In this paper, a compact ultra-wideband (UWB) band-pass filter (BPF) with a single narrow notched band is proposed. This filter is designed using a novel multiple-mode resonator (MMR) based on a grounded circular patch resonator (GCPR). The proposed MMR generates three main resonances and two transmission zeros (TZs). A semi-lozenge slot (SLS) is proposed to control resonant frequencies and obtain UWB operation. The 3dB notched band is achieved from 5.65–5.8 GHz by connecting an arrowhead stub inside the filter. The UWB filter has been simulated, fabricated and measured. The dimension of the designed filter is about  $0.31 \times 0.31 \lambda_g \times \lambda_g$ .

**Keywords:** band-pass filter; BPF; circular patch resonator; compact; ultra-wideband; UWB; notched band.

**Reference** to this paper should be made as follows: Shavakand, M.Y. and Ahmadi-Shokouh, J. (2019) ‘Compact UWB filter with narrow notched band based on grounded circular patch resonator’, *Int. J. Ultra Wideband Communications and Systems*, Vol. 4, No. 1, pp.16–21.

**Biographical notes:** Mona Yazdani Shavakand is a Master student at the Faculty of Electrical and Computer Engineering, University of Sistan and Baluchestan, Zahedan, Iran.

Javad Ahmadi-Shokouh received his BS degree in Electrical Engineering from Ferdowsi University of Mashad, Mashad, Iran, in 1993, MS degree in Electrical Engineering from the University of Tehran, Tehran, Iran, in 1995, and PhD degree in Electrical Engineering from the University of Waterloo, Waterloo, ON, Canada, in 2008. He is currently with the Department of Electrical Engineering, University of Sistan and Baluchestan, Zahedan, Iran, as an Associate Professor. His research interests are antenna and microwave for all applications, RF-baseband co-design for wireless communication systems, millimeter wave and ultrawideband (UWB) systems, smart antennas.

---

### 1 Introduction

Since Federal Communication Commission (FCC) (2002) has released the 3.1 to 10.6 GHz band as unlicensed band, a tremendous interest to the development of ultra-wideband (UWB) systems have been aroused. The UWB band-pass filter (BPF) has essential role in UWB communication system and influences the overall its performance. Various methods have been utilised to achieve UWB BPF such as compositing right/left-handed concept (Ahmad and Virdee, 2013), parallel-coupled lines (Abbosh, 2012) and multiple-mode resonator (MMR) (Song and Xue, 2010; Chiou et al., 2006; Feng et al., 2013, 2014; Janković et al., 2016). The ordinary MMR are realised based on stub-loaded line (Song and Xue, 2010), stepped impedance resonator (Chiou et al., 2006), ring resonator (Feng et al., 2013) or cross-shaped resonator (Feng et al., 2014). Although most of those filter have good performance, but they suffer from

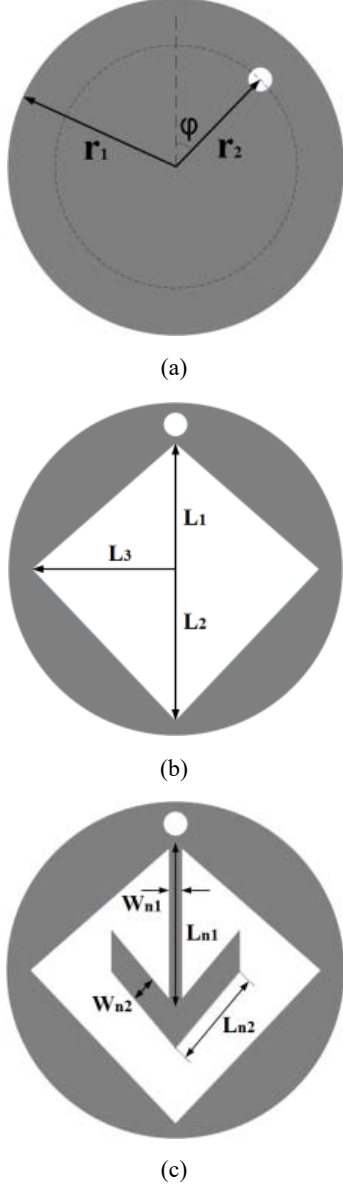
large group delay and lack of compactness. Moreover, they have low power-handling capability because of transmission line substantial. To overcome these shortcomings, a square patch resonator has been preferred to design UWB BPF in Janković et al. (2016). However, this filter cannot avoid undesired band.

Un-wanted interference in UWB band caused by co-existing wireless system can be eliminate with different techniques like defected grounded structure (DGS) (Li et al., 2010), electromagnetic band gap (EBG) (Liu et al., 2011), stub-loaded resonator (Xu et al., 2012). These techniques often cause increasing dimensions and insertion loss. Also they don't assure narrow notched band.

In this paper, a novel UWB BPF with a narrow notched band is realised based on grounded circular patch resonator (GCPR). The configuration of the proposed MMR is shown in Figure 1. This filter is based on patch resonator thus has a higher power-handling capability than transmission line

based filters. The semi-lozenge slot (SLS) can conveniently locate the required resonant frequencies in UWB band and creates free area inside the patch for connecting arrowhead stub. Hence, the undesired band can be avoided without increasing overall size. This filter is very compact and low profile. In addition, it has good in-band performance, low group delay and one narrow notched band.

**Figure 1** Geometry of proposed MMR, (a) GCPR (b) GCPR with SLS (c) GCPR with SLS and arrowhead stub



The rest of this paper is organised as follows: in Section 2, the multimode behaviour of the GCPR is theoretically analysed for locating via place. Then in Section 3, the resonant frequencies are controlled by SLS to obtain UWB performance. The arrowhead stub is tuned to achieve narrow notched band in Section 4. Finally, the simulation and measurement results are investigated in Section 5 and the conclusion of the paper is presented in Section 6.

## 2 Theoretical analysis

The proposed MMR is constructed based on GCPR. When a circular patch is grounded with via, a series inductance with the static capacitance of the patch is generated and this issue causes that some new resonant modes occur (Xu et al., 2000). These so-called symmetric modes create multiple-mode behaviour for patch. Thus, the GCPR is a good candidate to cover UWB frequency rang by appropriate tuning.

Figure 1(a) shows the geometry of GCPR. According to this architecture, a circular patch of radius  $r_1$  is loaded with a passive conducting post of radius  $\Delta$  at angular location  $\varphi$  on the circumference of a concentric circle of radius  $r_2$ , where  $r_2 < r_1$ . In Chakravarty and De (1999), a theoretical analysis based on cavity model method is performed to calculate resonant frequencies of a circular patch with multi shorting-post. When circular patch is loaded with a single thin via at  $\varphi=0^\circ$  then the equations in Chakravarty and De (1999) are simplified as:

$$\frac{J'_n(t_1 x_{nm}) Y'_n(x_{nm}) - J'_n(x_{nm}) Y'_n(t_1 x_{nm})}{J_n(t_1 x_{nm}) Y_n(x_{nm}) - J_n(x_{nm}) Y_n(t_1 x_{nm})} = \frac{J'_n(t_1 x_{nm})}{J_n(t_1 x_{nm})} = \begin{cases} \frac{\varepsilon_n}{t_1 x_{nm} L_n\left(\frac{t_2}{x_{nm}}\right)}, & \text{Symmetric-Mode} \\ 0, & \text{Asymmetric-Mode} \end{cases} \quad (1)$$

where

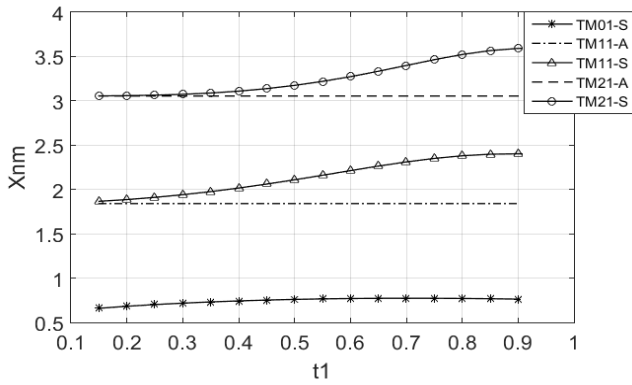
$$t_1 = \frac{r_2}{r_1}, \quad t_2 = \frac{r_1}{\Delta}, \quad \varepsilon_n = \begin{cases} 1, & n = 0 \\ 2, & n \neq 0 \end{cases}$$

$J_n$  and  $Y_n$  are Bessel function of the first and second kind, respectively. The Eigenvalue,  $x_{nm}$ , for  $TM_{nm}$  mode is obtained by solving (1). Where  $n$  denotes the order of the Bessel function and  $m$  corresponds to the  $m^{\text{th}}$  zero of (1). Then resonant frequency can be calculated by:

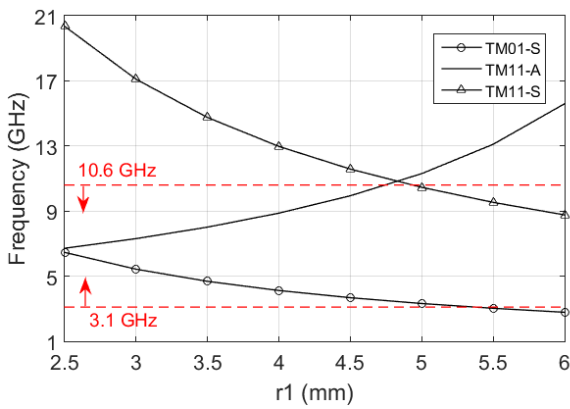
$$f_{nm} = \frac{x_{nm} 300}{2\pi r_1 \left[ \varepsilon_r \left\{ 1 + \frac{2h}{\pi r_1 \varepsilon_r} \left[ L_n\left(\frac{\pi r_1}{2h}\right) + 1.7726 \right] \right\} \right]^{1/2}} \quad (2)$$

Figure 2 displays the eigenvalues against the variations of  $t_1$ , while  $t_2 = 20$  is assumed. When  $t_1$  increases, the eigenvalues of  $TM_{11}$  asymmetric mode are constant because of independence of  $t_1$ . By increasing  $t_1$ , the eigenvalues of the  $TM_{11}$  symmetric mode increase and the eigenvalues of the  $TM_{01}$  symmetric mode are almost constant. Thus  $t_1 = 0.9$  is selected to achieve the widest bandwidth. Figure 3 shows the resonant frequencies against the variations of  $r_1$ , while  $t_1 = 0.9$  and  $t_2 = 20$  are assumed. By choosing  $r_1 = 4\text{mm}$ , the low dimension constraint is achieved; however, the resonances don't occur in correct frequencies.

**Figure 2** Investigation of the eigenvalues against the variations of  $t_1$



**Figure 3** Investigation of resonant frequencies against the variations of  $r_1$  (see online version for colours)



### 3 UWB filter without notched band

In this section, three types of slots are proposed and investigated to control resonant frequencies. Each of these slots can be used to achieve UWB filtering operation, but their tuning processes are different. The circle slot in Figure 4(a) has one degree of freedom (radius) to design and cannot control resonant frequencies independently. Thus, the circle slot is not a good candidate. The cross shaped slot in Figure 4(b) can control resonant frequencies independently, but it does not create free area inside GCPR. When notched band behaviour is desired, a stub should be placed outside GCPR, and consequently the overall size will be increased. The demonstrated SLS in Figure 4(c) has three degrees of freedom which can be enlisted for tuning. It can decrease resonant frequencies consciously and almost independently and also create free area inside GCPR.

The SLS architecture is made of two isosceles triangular slots which are connected together from their bases. Figure 5(a) reveals triangular slots can't make a useful impact on the resonances, especially on the second resonance. However, when they are connected to each other, the second resonance is significantly reduced. By increasing the vertical diameter of SLS, the second resonance decreases. Lastly, the second resonance is located near the central frequency of UWB band by choosing  $L_1 = 2.8\text{mm}$  and  $L_2 = 3.7\text{mm}$ .

**Figure 4** The GCPR with (a) circular slot, (b) cross shaped slot and (c) SLS

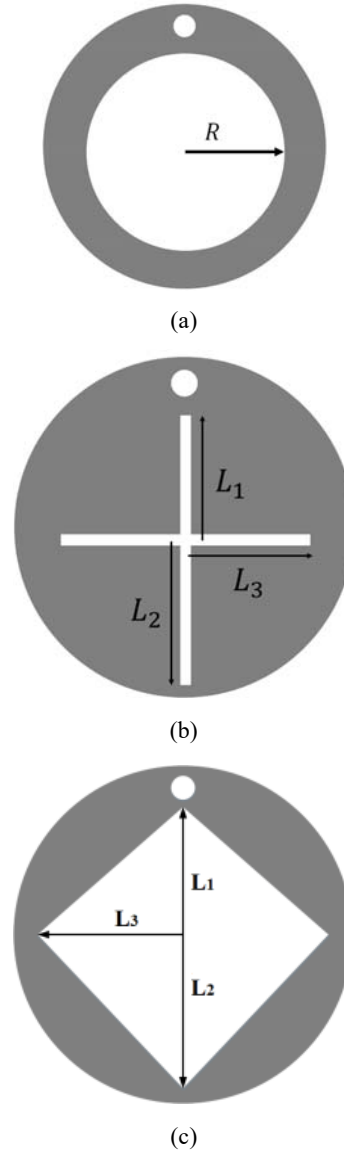


**Figure 5**  $|S_{21}|$  under weak coupling, (a) comparison of triangular slots and SLS (b) variation the horizontal diameter of SLS (see online version for colours)

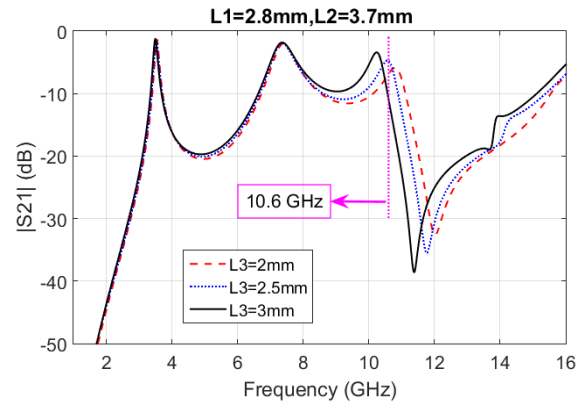


Figure 5(b) demonstrates resonant frequencies variation for different dimensions of  $L_3$ . The horizontal diameter of SLS is used to set third resonance at the correct frequency. When

this diameter is increased, the third resonance is decreased and entered in passband. Moreover, the out of band TZ decreases by increasing of  $L_3$  and thus selectivity increases.

#### 4 UWB filter with notched band

An arrowhead stub is proposed in this paper to avoid the interferences such as WLAN signals. The configuration of this stub is shown in Figure 6. It is a step-impedance resonator inherently, that minimised and folded to be embedded inside filter and create notched band property without increasing dimension. The input impedance of the arrowhead stub is calculated by:

$$Z_{in} = \frac{K \tan \theta_1 - \cot \theta_2}{K + \tan \theta_1 \cot \theta_2} \quad (3)$$

where  $\theta_1$  and  $\theta_2$  are the electrical lengths of two section and  $K = Z_1 / Z_2$  is the stepped-impedance ratio of the arrowhead stub.

**Figure 6** Geometry of the arrowhead stub

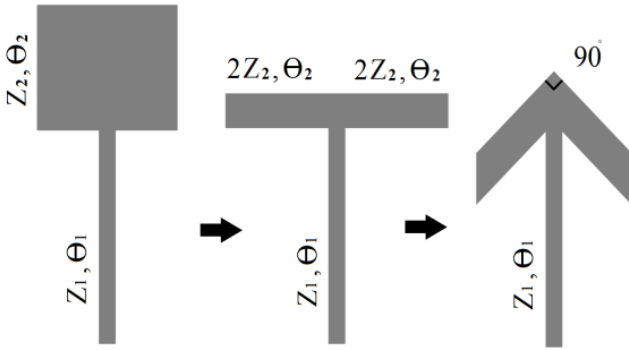


**Figure 7** Investigation of the added resonant frequency and in-band TZ against the variations of (a)  $L_{n1}$  and  $W_{n2}$  and (b)  $L_{n1}$  and  $W_{n1}$  (see online version for colours)

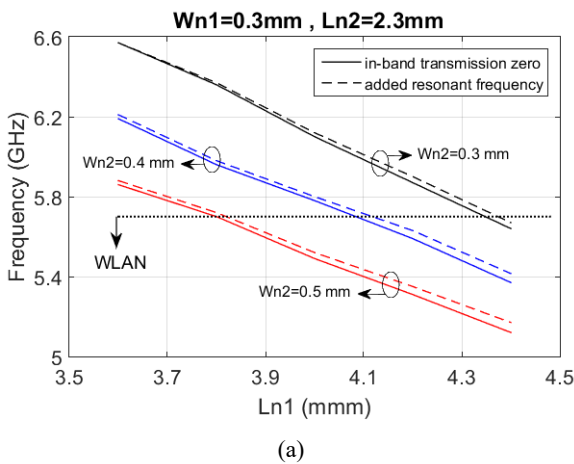
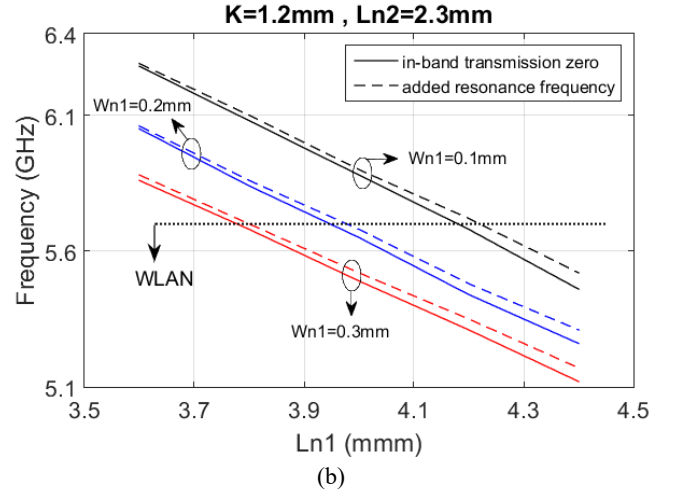


**Figure 7** Investigation of the added resonant frequency and in-band TZ against the variations of (a)  $L_{n1}$  and  $W_{n2}$  and (b)  $L_{n1}$  and  $W_{n1}$  (continued) (see online version for colours)

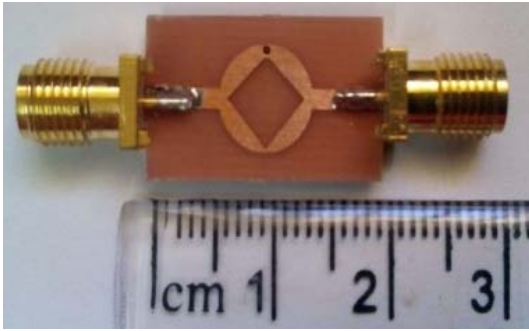


The arrowhead stub adds a resonant frequency and an in-band TZ to filter. Figure 7(a) demonstrates when  $W_{n2}$  increases, the added resonant frequency and in-band TZ occur for the lower  $L_{n1}$ . Hence  $W_{n2} = 0.5\text{mm}$  caused the arrowhead stub can eliminate WLAN band by minimised dimension. To achieve narrow notched band, an intelligent tuning is used in Figure 7(b). At first,  $K = 1.2$  is assumed constant to omit the effect on results. Then the variations of added resonant frequency and near in-band TZ against  $W_{n1}$  and  $L_{n1}$  are investigated. Figure 7(b) shows by increasing  $W_{n1}$ , the added resonant frequency and in-band TZ occur for the lower  $L_{n1}$ . Also they are located near each other and thus, a narrow band can be achieved. Therefore  $W_{n1} = 0.3\text{mm}$  is chosen to create narrow notched band with minimised dimension.

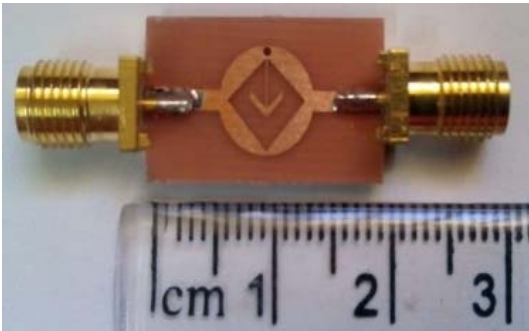
#### 5 Results and discussions

To create UWB filter, the feed lines are connected to the proposed MMR with  $180^\circ$  angle. The dimensions of proposed UWB filters are  $r_1 = 4$ ,  $r_2 = 3.6$ ,  $\Delta = 0.2$ ,  $W_{n1} = 0.3$ ,  $W_{n2} = 0.5$ ,  $L_1 = 2.8$ ,  $L_2 = 3.7$ ,  $L_3 = 3$ ,  $L_{n1} = 3.8$  and  $L_{n2} = 2.3$ . Figure 8 displays the Photograph of the fabricated filters. The notched band operation is achieved without increasing overall dimensions and the proposed filters are compact in size, i.e., about  $0.31 \times 0.31 \lambda_g \times \lambda_g$ . The measurement results of S-parameters in Figure 9 illustrate good agreement with simulation results. The proposed filters are fabricated on FR4 because of low cost. If they are fabricated on better substrate, the better agreement between simulation and measurement results will be obtained.

**Figure 8** Photograph of fabricated UWB filter, (a) without notched band (b) with notched band (see online version for colours)



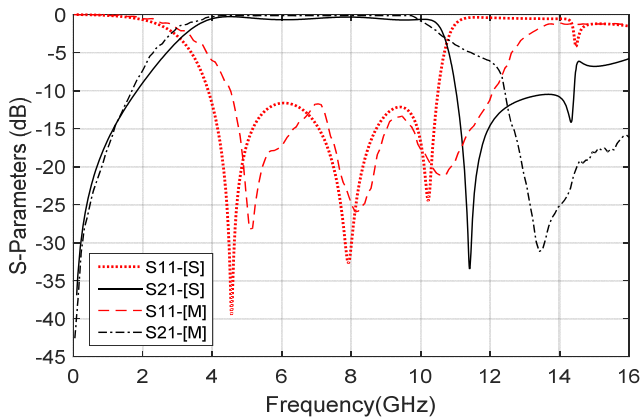
(a)



(b)

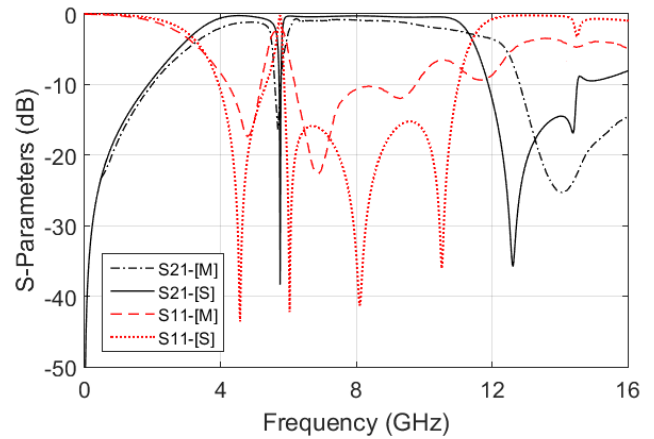
Figure 9(a) shows the return loss of the UWB filter without notched band is better than 12 dB and insertion loss is 0.32 dB in passband. Thus, this filter has a good in-band performance and the fractional 3-dB bandwidth is 110% (3.05GHz-10.6GHz). When the arrowhead stub is connected, the UWB filter can eliminate WLAN band with NFBW=1.75%. According to Figure 9(b), the UWB filter with notched band has return loss better than 10 dB and insertion loss is 0.55 dB in pass-band. The fractional 3-dB bandwidth of the UWB filter with notched band is 126% (3.15GHz-11.8GHz).

**Figure 9** The comparison of measurement and simulation results, (a) UWB filter without notched band (b) UWB filter with notched band (see online version for colours)



(a)

**Figure 9** The comparison of measurement and simulation results, (a) UWB filter without notched band (b) UWB filter with notched band (continued) (see online version for colours)



(b)

The group delay of the UWB filters with and without notched band is shown in Figure 10. Their group delays are adequately flat between 0.22-0.25 (ns). The UWB filters are compared with previous works in Table 1. This table demonstrates the proposed filters have compact size, low group delay and better in-band operation than other filters.

**Figure 10** Group delay (see online version for colours)

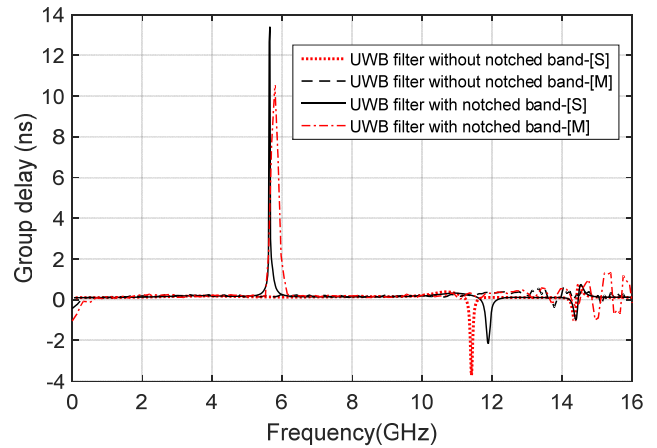


**Table 1** Comparison between the proposed UWB filter and previous works

Ref.	Size ( $\lambda_g \times \lambda_g$ )	IL (dB)	RL (dB)	FBW (%)	GDV (ns)	NFBW (%) @ 5.7
Ahmad and Virdee (2013)	$0.52 \times 0.15$	0.5	11	115	0.5	1.75 (10-dB) @ 5.7
Abbosh (2012)	$1.03 \times 0.73$	1	20	110	0.12	-
Feng et al. (2013)	$0.35 \times 0.19$	0.95	14	126	0.22	7 (10-dB) @ 5.7
Li et al. (2010)	$0.46 \times 0.14$	1.6	13	125	0.5	18.5 (3-dB) @ 5.4
Liu et al. (2011)	$0.97 \times 0.3$	-	13	112	0.25	3.4 (10-dB) @ 5.8
This work	$0.31 \times 0.31$	0.55	14	126	0.22	1.75 (10-dB) @ 5.7

## 6 Conclusions

In this paper, a compact UWB BPF with single narrow notched band is designed based on GCPR. Incorporating a single shorting post significantly reduces the overall size of filter. The UWB frequency response is achieved by a SLS. Avoiding WLAN band is also characterised by an arrowhead stub. The proposed filters can be used for UWB systems where in-band performance is more important than out-of-band performance. Moreover, these filters are appropriate when the immunity of the phase of signal is significant.

## References

- Abbosh, A.M. (2012) 'Design method for ultra-wideband band-pass filter with wide stopband using parallel-coupled microstrip lines', *IEEE Trans. Microw. Theory Tech.*, January, Vol. 60, No. 1, pp.31–38.
- Ahmad, K.U. and Virdee, B.S. (2013) 'Ultra-wideband band-pass filter based on composite right/left handed transmission-line unit-cell', *IEEE Trans. Microw. Theory Tech.*, February, Vol. 61, No. 2, pp.782–788.
- Chakravarty, T. and De, A. (1999) 'Design of tunable modes and dual-band circular patch antenna using shorting posts', *IEE Proc. – Microw., Antennas and Propag.*, June, Vol. 146, No. 3, pp.224–228.
- Chiou, Y.-C., Kuo, J.-T., Cheng, E. (2006) 'Broadband quasi-chebyshev band-pass filters with multimode stepped-impedance resonators (SIRs)', *IEEE Trans. Microw. Theory Tech.*, August, Vol. 54, No. 8, pp.3352–3358.
- Federal Communications Commission (2002) *Revision of Part 15 of the Commission's Rules Regarding Ultra-Wideband Transmission Systems*, First Note and Order Federal Communications Commission, ET-Docket, pp.98–153.
- Feng, W., Che, W. and Xue, Q. (2013) 'Compact ultra-wideband band-pass filters with narrow notched bands based on a ring resonator', *IET Microw. Antenna and Propag.*, September, Vol. 7, No. 12, pp.961–969.
- Feng, W., Che, W., Xue, Q. (2014) 'Design of ultra-wideband band-pass filters with fixed and reconfigurable notch bands using terminated cross-shaped resonators', *IEEE Trans. Microw. Theory Tech.*, February, Vol. 62, No. 2, pp.252–265.
- Janković, N., Niarchos, G., Crnojević-Bengin, V. (2016) 'Compact UWB band-pass filter based on grounded square patch resonator', *Elec. Lett.*, February, Vol. 52, No. 5, pp.372–374.
- Li, Q., Li, Z.-J., Liang, C.-H. and Wu, B. (2010) 'UWB band-pass filter with notched band using DSRR', *Elec. Lett.*, May, Vol. 46, No. 10, pp.692–693.
- Liu, B.-W., Yin, Y.-Z., Yang, Y., Jing, S.-H. and Sun, A.-F. (2011) 'Compact UWB band-pass filter with two notched bands based on electromagnetic bandgap structures', June, *Elec. Lett.*, Vol. 47, No. 13, pp.757–758.
- Song, K. and Xue, Q. (2010) 'Inductance-loaded y-shaped resonators and their applications to filters', *IEEE Trans. Microw. Theory Tech.*, April, Vol. 58, No. 4, pp.978–984.
- Xu, J., Wu, W., Kang, W., Miao, C. (2000) 'Theory of miniaturized shorting-post microstrip antennas', *IEEE Trans. Antennas Propag.*, January, Vol. 48, No. 1, pp.206–208.
- Xu, J., Wu, W., Kang, W., Miao, C. (2012) 'Compact UWB band-pass filter with a notched band using radial stub loaded resonator', *IEEE Microw. Wireless Compon. Lett.*, Vol. 22, No. 7, pp.206–208.